Exploiting FDD Channel Reciprocity for Physical Layer Secret Key Generation in IoT Networks

Ehsan Olyaei Torshizi, and Werner Henkel, *Senior Member, IEEE*

***Abstract*—The utilization of physical layer Secret Key Generation (SKG) is increasingly prevalent in securing wireless communication within Internet of Things systems, particularly in Narrow-band IoT. While most key-generation schemes are tailored for Time Division Duplex (TDD) systems, generating secret keys in Frequency Division Duplex (FDD) systems presents challenges due to the distinct frequency bands for uplink and downlink. In response to this, we propose an efficient FDD-based key generation technique that capitalizes on the reciprocity of scattering matrix parameters S_{12} and S_{21} within the same frequency range. Specifically, we harness the capabilities of MUSIC algorithm during the direction of arrival estimation phase. Numerical results demonstrate promising outcomes in addressing key challenges, including randomness, and Key Disagreement Ratio (KDR).**

***Index Terms*—Secret key generation, FDD, IoT, direction of arrival, MUSIC, physical layer.**

I. Introduction

The Internet of Things (IoT) is driving a profound transformation in our lives, seamlessly connecting people, environments, and machines [1]. As IoT applications frequently involve sensitive data, ensuring its safeguard is imperative for maintaining privacy and security. A majority of IoT devices rely on wireless connectivity, such as WiFi, IEEE 802.15.4 (ZigBee), Bluetooth, NB-IoT, LoRa, and Sigfox. Yet, the vulnerability of wireless channels to eavesdropping and intervention introduces the risk of unauthorized access through a tuned receiver within a specific signal-to-noise ratio (SNR) range. The swift proliferation of IoT applications accentuates the urgency of addressing potential data security gaps, as they can undermine societal trust in IoT services.

Recent attention has been directed towards physical layer secret key generation (SKG) due to its potential to establish secure and efficient keys in wireless communication systems. These algorithms derive secret keys based on wireless channel characteristics, making them unique and formidable for potential attackers to acquire. Effective pairwise key generation necessitates a high degree of similarity in channel features between two authorized users. In frequency division duplexing (FDD) systems, where uplink and downlink transmissions occur in separate frequency bands with distinct fading, challenges arise due to the lack of alignment in mutually attainable channel parameters between the uplink and downlink. This misalignment poses a challenge in identifying frequency-independent reciprocal channel parameters for FDD systems. Given that most wireless systems, including 5G networks, Long Term Evolution (LTE), and narrowband IoT, rely on FDD, addressing this open problem is crucial.

Presently, key generation for FDD systems has been explored in a limited number of publications. In [2], the Separating - Adjusting - Reconstructing (SAR) framework is proposed, involving channel path separation, carrier frequency-based adjustment, and final path amplitude and phase reconstruction. Notably, separating channel paths in a complex multipath environment presents challenges. [3] introduces a SKG method using angle and path delay, while [4] presents a key generation approach based on the reciprocity of channel covariance matrix eigenvalues, requiring a specific antenna array configuration. Loopback-based key generation approaches, outlined in [5] and [6], aim to establish a channel with reciprocal channel gain, incorporating an additional reverse channel training phase for key generation. However, these schemes face challenges such as a high risk of eavesdropping and substantial channel detection complexity [7]. In parallel with model-based strategies, recent advancements include deep learning-based approaches [8]. However, these schemes are notably dependent on the specific environment, as the models can only discern the feature mapping function within a given context. The challenge arises from the need to accumulate data and train models for individual communication environments, requiring significant resources and training data. Consequently, the practical applicability of these methodologies in real-world scenarios becomes limited. In [9], we demonstrated, to the best of our knowledge, for the first time, that FDD exhibits a usable symmetry concerning the direction of arrival [10]. To further improve and leverage channel reciprocity in FDD systems, this letter introduces an innovative SKG scheme that capitalizes on reciprocity within the same frequency range to generate similar keys. Our contributions are outlined below:

- Introduction of the direction of arrival, derived from bidirectional measurements of scattering parameters S_{12} and S_{21} as a reciprocal channel parameter for key generation.
- Proposal of a novel secret key generation scheme tailored for FDD systems, establishing highly correlated keys with a low disagreement ratio.
- Introduction of a straightforward yet highly effective concept of one-sided centering key reconciliation, significantly reducing the key disagreement ratio (KDR).

II. System model and Scattering parameters

We considered the basic key generation model, in which Alice and Bob create secure keys based on channel state information (CSI). In addition, an adversary, Eve, monitors

E. Olyaei Torshizi and W. Henkel are with the School of Computer Science and Engineering, Constructor University, Bremen, 28759, Germany. Emails: eolyaei@constructor.university and werner.henkel@ieee.org (This work was funded by the Deutsche Forschungsgemeinschaft (DFG, German Research Foundation) - HE 3654/27-1.)

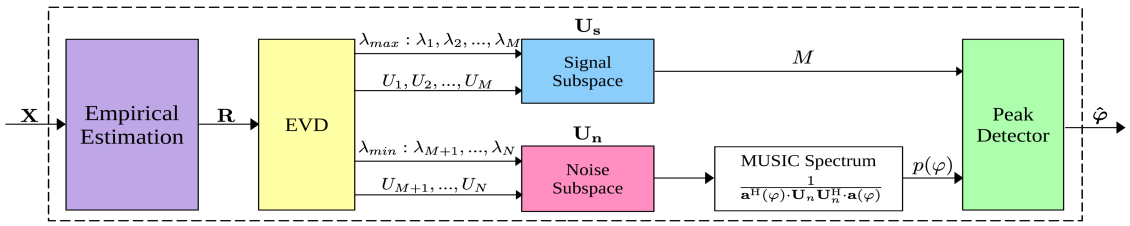

Fig. 1: Block diagram of the DoA estimation process using the MUSIC algorithm

communications during key generation, aiming to intercept the keys. To prevent correlation between the legal channel $A \to B$ and the wiretap channels $A \to E$ and $B \to E$, it is assumed that Eve is positioned far enough away from Alice and Bob.

For a 2-port RF network, the S-parameter matrix describes the relationship between the incident (a_1 and a_2) and reflected (b_1 and b_2) wave parameters as follows:

$$\begin{bmatrix} b_1 \\ b_2 \end{bmatrix} = \begin{bmatrix} S_{11} & S_{12} \\ S_{21} & S_{22} \end{bmatrix} \begin{bmatrix} a_1 \\ a_2 \end{bmatrix} , \tag{1}$$

where S_{11} and S_{22} represent the self-reflection factors, S_{12} and S_{21} signifies the forward and reverse transmission factors, respectively. A network is considered reciprocal if $S_{12} = S_{21}$. This reciprocity holds for every passive two-port, and in the context of wireless communication, a channel along with connecting cables can be treated as a two-port system.

III. DoA Estimation

Direction of arrival/departure (DoA/DoD) estimation algorithms rely on phase or delay differences of received signals at different antennas, thus requiring at least two antennas in an array. The data model for an arbitrary array structure consisting of N sensor elements measuring M impinging narrowband signals, corrupted by noise takes the following form

$$\mathbf{x} = \mathbf{A}\mathbf{s} + \mathbf{n} , \tag{2}$$

where $\mathbf{s} = [s_1\ s_2\ \dots\ s_{\mathrm{M}}]^{\mathrm{T}}$ is considered as source signals, and the matrix $\mathbf{A} = [\mathbf{a}(\varphi_1)\ \mathbf{a}(\varphi_2)\ \dots\ \mathbf{a}(\varphi_{\mathrm{M}})]$ is an $N \times M$ matrix of the M steering vectors. Moreover, $\mathbf{a}(\varphi)$ represents the steering vector of the signal whose direction we are attempting to estimate, and the goal is estimating φ_m, $m = 1, ..., M$.

A. MUSIC Algorithm

The Multiple Signal Classification (MUSIC) algorithm [11] is a popular spectral estimation technique widely used in signal processing applications. It operates by utilizing an array of sensors, such as antennas, to extract spatial information from a signal source. The algorithm takes as input K snapshots of the waveforms at N array elements, represented as $\mathbf{x}$ in (2), and uses them to obtain an empirical estimate of $\mathbf{R}$ via $\hat{\mathbf{R}}_{\mathbf{x}} = \frac{1}{K}\sum_{k=1}^{K} \mathbf{x_k}\mathbf{x_k}^{\mathrm{H}}$. The eigenvectors corresponding to the $N - M$ smallest eigenvalues form the noise subspace $\mathbf{U_N}$, which is orthogonal to the M dimensional signal subspace spanned by the incident signal mode vectors. Moreover, λ_{min} and λ_{max} are corresponding to minimal and maximal eigenvalues of $\hat{\mathbf{R}}_{\mathbf{x}}$, respectively. The corresponding block diagram in Fig. 1 illustrates the structure of the MUSIC algorithm.

The received signal E_s of one source component $s(t)$ can be considered as

$$E_s(t, \mathbf{r}) = s(t)e^{j(\omega t - \mathbf{r}^T\mathbf{k})} , \tag{3}$$

in which $\mathbf{r}$ denotes the position of the receiving antenna (also transmitting antenna due to reciprocity) and $\mathbf{k}$ is the wave number which can be expressed by

$$\mathbf{k} = k(\cos\varphi, \sin\varphi)^{\mathrm{T}}, \quad k = \frac{\omega}{c} . \tag{4}$$

In case of a circular array with N antennas and the antenna index n, we express

$$\mathbf{r}_n = R \cdot \big(\cos(2\pi\frac{(n-1)}{N}), \sin(2\pi\frac{(n-1)}{N})\big)^{\mathrm{T}} , \tag{5}$$

Substituting (4) and (5) inside (3) yields the exponential function as

$$a_n = e^{-j\frac{2\pi}{\lambda}R\cos(\varphi - 2\pi\frac{n-1}{N})}, \quad n = 0, ..., N-1 . \tag{6}$$

This is a component of the so-called steering vector $\mathbf{a}$. When computing the spatial correlation matrix

$$\begin{aligned}\mathbf{R} &= \mathrm{E}\{\mathbf{x}(t)\mathbf{x}(t)^{\mathrm{H}}\} = \mathbf{A}\mathrm{E}\{\mathbf{s}(t)\mathbf{s}(t)^{\mathrm{H}}\}\mathbf{A}^{\mathrm{H}} + \mathrm{E}\{\mathbf{n}(t)\mathbf{n}(t)^{\mathrm{H}}\} \\ &= \mathbf{U}\mathbf{\Lambda}\mathbf{U}^{\mathrm{H}} = \mathbf{U}_S\mathbf{\Lambda}_S\mathbf{U}_S^{\mathrm{H}} + \mathbf{U}_N\mathbf{\Lambda}_N\mathbf{U}_N^{\mathrm{H}} ,\end{aligned} \tag{7}$$

which consists of signal and noise components. $\mathbf{x}(t)$ is the received vector of length N, $\mathbf{s}$ denotes a source vector of M components, and $\mathbf{n}$ is a noise vector of length N. The so-called MUSIC spectrum is expressed as

$$P_{\mathrm{MUSIC}}(\varphi) = \frac{1}{\mathbf{a}^{\mathrm{H}}(\varphi)\cdot\mathbf{U}_N\mathbf{U}_N^{\mathrm{H}}\cdot\mathbf{a}(\varphi)} . \tag{8}$$

The steering vector $\mathbf{a}$ is dependent of the angle φ. The maxima of the MUSIC spectrum will be obtained at angles where the steering vector is orthogonal to the noise eigenvectors. A stepwise pseudo-code provided as Algorithm 1 comprehensively explains the steps of the MUSIC algorithm.

Algorithm 1 DoA Estimation using MUSIC

Input: Measured vector $\mathbf{X}$ (in our case S-parameters from Alice's ($\mathbf{X}_A = \mathbf{S}_{12}$) and Bob's ($\mathbf{X}_B = \mathbf{S}_{21}$) sides), number of sources M, total number of sensors N

Output: Estimated directions of arrival $\hat{\varphi}_m$, $m = 1, ..., M$

1. Estimate the correlation matrix $\mathbf{R}$ from the received data $\mathbf{R} \leftarrow \frac{1}{K}\mathbf{x}\mathbf{x}^H$
2. Perform eigendecomposition $\mathbf{R} = \mathbf{U}\mathbf{\Lambda}\mathbf{U}^H$
3. Partition $\mathbf{U}$ to obtain noise subspace, matrix $\mathbf{U}_N$, corresponding to the $(N - M)$ smallest eigenvalues of $\mathbf{U}$
4. Generate steering vectors $\mathbf{a}(\varphi)$ for a range of directions φ
5. Compute the MUSIC spectrum using Eq. (8)
6. Identify peaks in $P_{\mathrm{MUSIC}}(\varphi)$ as estimated DoA

IV. Proposed SKG Scheme

This section provides a detailed description of the proposed SKG. As depicted in Fig. 2, the key generation procedure comprises four steps:

- **Channel Probing and DoA Estimation:** In our experimental setup, Alice is configured as an antenna array, while Bob and Eve are equipped with single dipoles. In this phase, Alice and Bob initially collect datasets in a wireless environment by measuring S-parameter vectors $\mathbf{S_{12}}$ and $\mathbf{S_{21}}$. These measurements are conducted between Bob's single dipole and each antenna within Alice's array. It is important to note that for each measurement round, only one antenna on Alice's side is activated, while the remaining antennas are kept inactive. This approach ensures that each measurement round yields a unique set of $\mathbf{S_{12}}$ and $\mathbf{S_{21}}$ vectors, representing the interaction between Bob and a specific antenna in Alice's array. This procedure is repeated to cover all N antennas on Alice's side, thereby acquiring N distinct $\mathbf{S_{12}}$ and $\mathbf{S_{21}}$ vectors (over frequency samples) for the interactions between Bob and Alice. Evidently, measured results are identical for both transmit directions due to reciprocity. This consistency implies that the DoA coincides with the DoD. In order to construct the channel profiles, we conducted measurements of $\mathbf{S_{12}}$ and $\mathbf{S_{21}}$ at two distinct dedicated neighboring $\Delta f = 5$ MHz frequency bands on either side of a central frequency of $f_c = 2.1925$ GHz. Specifically, we designate the link from Bob to Alice for measuring $\mathbf{S_{12}}$ and constructing $\mathbf{X_A}$. Similarly, the link from Alice to Bob is assigned for measuring $\mathbf{S_{21}}$ and constructing $\mathbf{X_B}$. Both $\mathbf{S_{12}}$ and $\mathbf{S_{21}}$ separately consist of N frequency samples obtained over FDD bands I and II, respectively. Subsequently, the DoA and DoD angles between Bob and each antenna on Alice's side will be estimated using the MUSIC algorithm on both sides.
- **Quantization:** In this stage, phase estimates from both sides, $\hat{\varphi}_{\mathrm{A}}$ and $\hat{\varphi}_{\mathrm{B}}$, are quantized into an M-bit vector, using Gray mapping, to generate primary keys. We use linear quantization to divide the entire $0 \leq \alpha \leq \alpha_{max}$ phase range ($\alpha_{\max} = 2\pi$ for azimuth and $\alpha_{\max} = \pi$ for elevation) into 2^M equal quantization intervals as $[\alpha_{max}(i-1)/2^M, \alpha_{max} i/2^M)$, $1 \leq i \leq 2^M$. Subsequently, based on $\hat{\varphi}_{\mathrm{A}}$ and $\hat{\varphi}_{\mathrm{B}}$, the corresponding quantization intervals $\mathcal{Q}_{\mathrm{A}}$ and $\mathcal{Q}_{\mathrm{B}}$ for Alice and Bob, belonging to $\{1, 2, ..., 2^M\}$, can be determined by

$$\mathrm{Q}(\hat{\varphi}_{\mathrm{A/B}}) = \mathcal{Q}\,, \quad \text{if} \quad \mathrm{mod}\,(\hat{\varphi}_{\mathrm{A/B}}, \alpha_{\max}) \in \frac{\alpha_{\max}}{2^M}\left[(\mathcal{Q}-1)\,,\ \mathcal{Q}\right). \tag{9}$$

- **Key Reconciliation:** In this phase, it is imperative to identify and rectify quantization errors, commonly stemming from noise and hardware imperfections. To align and mitigate discrepancies in the generated initial keys due to quantization errors, a binary linear coding scheme such as Slepian-Wolf coding, based on BCH, Turbo, or LDPC codes, is commonly employed. To streamline the process and reduce computational overhead, we propose an initial non-coding approach, which is a simple yet effective one-sided centering idea for reconciliation. This method involves aligning the quantized measurements from one side (Alice or Bob) with the midpoint of the corresponding quantization interval and transmitting the necessary shift value to the other side. Therefore, based on obtained $\mathcal{Q}_{\mathrm{A}}$ and $\mathcal{Q}_{\mathrm{B}}$, the required shift to relocate $\hat{\varphi}_{\mathrm{A}}$ or $\hat{\varphi}_{\mathrm{B}}$ into the middle of its quantization interval can be determined by

$$\delta_{\mathrm{A/B}} = \hat{\varphi}_{\mathrm{A/B}} - \frac{\alpha_{\max}(2\mathcal{Q}_{\mathrm{A/B}} - 1)}{2^{M+1}}\,. \tag{10}$$

Then, this shift value will be communicated to the other side, and the resulting keys, $\mathbf{K}_A$ and $\mathbf{K}_B$, can be determined by applying it at both ends.
- **Privacy Amplification:** To eliminate information leakage during probing and reconciliation from potential eavesdropper Eve, privacy amplification synchronizes keys using Secure Hash Algorithms (SHA). SHA transforms data through complex hash functions, generating fixed-length, dissimilar strings, ensuring one-way functionality. In our study, SHA-256 and SHA-512 algorithms produced 64-bit and 128-bit privacy-amplified keys, respectively.

V. Simulation Results

This section evaluates the performance of the proposed SKG using the MUSIC algorithm, relying on actual measurement results. The evaluation is carried out in the context of a FDD system, with a central frequency fixed at 2.1925 GHz. Two contiguous 5 MHz frequency bands with and without band separation are examined for measuring S_{12} and S_{21}.

A. Testbed

We designed both uniform circular array (UCA) and uniform linear array (ULA) configurations at Alice's end. The UCA involves a rotatable disc with 40 antenna positions spaced approximately $\lambda/6$ apart, resembling an array with a radius of 14.568 cm. The corresponding ULA comprises 20 antenna positions with the same spacing, achieved through linear movement of the antenna plate along a straight path, remotely controlled. Scattering parameters S_{12} and S_{21} were measured using a standard vector network analyzer. To establish a comprehensive real dataset, we meticulously examined diverse indoor scenarios across 13 indoor environments, including offices, homes, labs, garages, basements, and

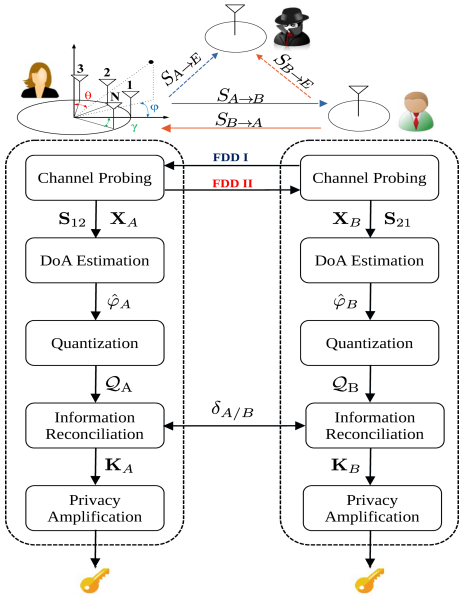

Fig. 2: The proposed secret key generation scheme

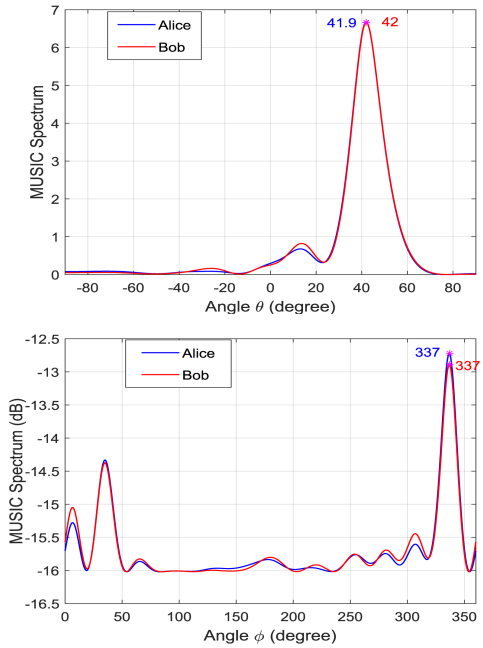

Fig. 3: 2D MUSIC spectra (azimuth), Top: ULA, Bottom: UCA

corridors. Exploring nearly 200 measuring scenarios for the UCA and 70 for the ULA, our investigations encompassed a spectrum of outcomes, from minimal to pronounced effects, such as scenarios with blocked paths or obstructed line-of-sight. Additionally, we varied the vertical positioning of Alice and Bob, capturing measurements in scenarios with both zero and nonzero height differences.

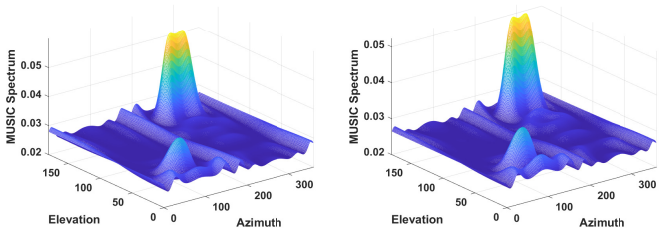

Fig. 4: 3D MUSIC spectra for UCA, Left: S_{12}, Right: S_{21}

B. Results

Consider a scenario in which Alice is positioned at a desk elevated 70 cm from the floor in one corner of a $7.5 \times 5.5 \times 3$ meter office with two windows and diverse items such as desks, monitors, laptops, printers, book shelves, cupboards, whiteboards, radiators, chairs, etc. At the diagonal opposite corner, Bob and Eve are situated maintaining a 0.5-meter distance between them. Figure 3 compares the respective 2D MUSIC spectra derived from the measurements of S_{12} and S_{21} for both UCA and ULA, separately. The peaks in the MUSIC spectra for both S_{12} and S_{21} correspond to the estimated DoAs for Alice and Bob, respectively. Our measurements and following computations are not restricted to azimuth only, but also include elevation. Figure 4 illustrates the corresponding 3D results for the measurement set presented in Fig. 3, specifically for the UCA. The nearly perfect alignment of both 2D and 3D MUSIC spectra obtained from S_{12} and S_{21} indicates complete reciprocity between Alice and Bob in both azimuth and elevation. This reciprocity ensures the generation of identical keys

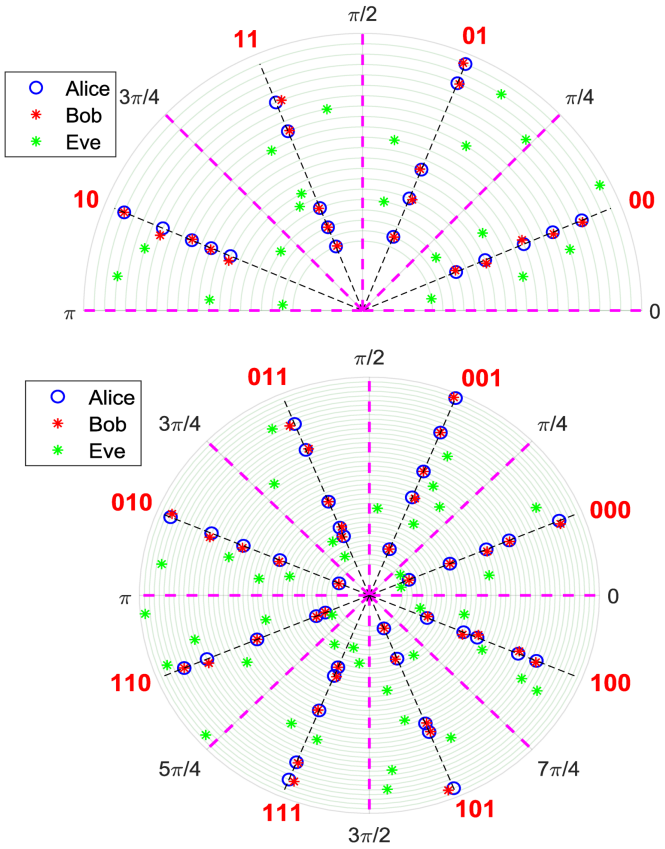

Fig. 5: Distribution of generated keys using MUSIC, Top: ULA, Bottom: ULC

for both parties. Figure 5 compares the position of reconciled version of estimated DoAs using the MUSIC algorithm for 20 and 40 different measurements, employing ULA and UCA, respectively. The illustration adopts a polar format, depicting the respective reconciled DoA phase positions at Alice, Bob, and Eve. The rings indicating the measurements (20 for ULA and 40 for UCA). Additionally, each sector of the circle is assigned to a specific quantization interval, separated by dashed purple lines. Utilizing two and three bits Gray mapping for ULA and UCA, respectively, the primary generated keys for each quantization interval are depicted in red. Figure 5 highlights the similarity of generated keys between Alice and Bob and the dissimilarity of the corresponding key at Eve for each measurement scenario.

The key disagreement ratio serves as a common metric for assessing key generation performance. It is defined as the average ratio of differing key bits between the Gray keys generated independently by Alice and Bob, divided by the total number of key bits. The averaged KDR of 2×10^{-5} was measured across all 200 scenarios for UCA and 70 scenarios for ULA, surpassing the values of 5×10^{-3} and 4×10^{-3} reported in [4] and [5], respectively, at an SNR of 10 dB. As another comparison, we employed the ESPRIT algorithm [12] for the DoA estimation under the same measurement scenarios, resulting in a KDR of 7×10^{-4}, indicating the superior performance of MUSIC. To assess the KDR in worst-case scenarios, deliberate obstructions such as steel doors were used along the line-of-sight (LoS) trajectory connecting the transmit and receive antennas. This intervention led to a deterioration

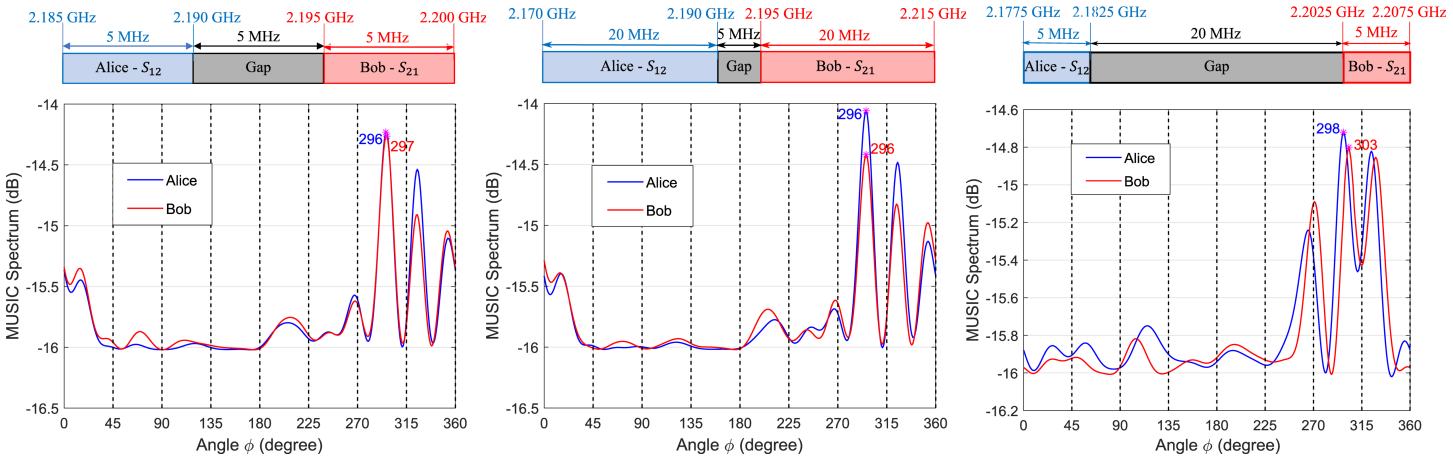

Fig. 6: 2D MUSIC spectra considering band separation and wider FDD bands for UCA

of the KDR to the 10^{-3} range. Additionally, we observed the averaged bit-wise KDR of 0.447 between the generated keys at Alice (or Bob) and the estimated keys at Eve. This is close to the theoretical ideal value of 0.5, equivalent to Eve flipping a coin for each bit.

The proposed SKG was validated by assessing the randomness of the generated secret key bits using the NIST test suite [13]. Due to bit length constraints, 9 representative tests out of the total 16 were conducted. All generated key bit sequences for both antenna arrays successfully passed the NIST test, as evidenced by P-values exceeding 0.01. Results are presented in Table I. The proposed FDD-based SKG approach relies on exploiting the proximity of corresponding frequency bands to utilize reciprocity for generating similar keys. However, we examined the results by varying frequency gaps between active FDD channels to evaluate key consistency between Alice and Bob across diverse scenarios. Additionally, wider FDD bands were also simulated to validate key consistency. The corresponding 2D MUSIC spectrum results for the UCA in the same measuring environment, considering both band separation and expanded FDD bands, are compared in Fig. 6. The vertical lines mark quantization intervals. The figure reveals that even with a 20 MHz gap between two active frequency bands, there is only a slight deviation in the estimated DoAs, falling within the same quantization interval and resulting in the generation of identical keys. Similar simulations confirm these findings for the ULA, as well.

TABLE I: NIST statistical test pass ratio (P-values)

Test	ULA	UCA
Approximate Entropy	0.7236	0.8011
Frequency (Monobit)	0.5312	0.5794
Frequency (within a block)	0.5544	0.6629
Cumulative sums (forward)	0.5061	0.5417
Cumulative sums (reverse)	0.3958	0.4153
Discrete Fourier Transform	0.6527	0.8351
Longest Run	0.2906	0.3438
Run	0.5720	0.6946
Serial	0.4991	0.6501

VI. Conclusion

In this letter, an innovative FDD-based physical layer security framework is introduced to enhance secure communications in IoT applications. This method exploits the inherent reciprocity between scattering parameters S_{12} and S_{21} of the legitimate partners within the same frequency range. Moreover, direction of arrival of bidirectional measurements (S_{12} and S_{21}) is estimated through the MUSIC algorithm, for both UCA and ULA. Numerical results demonstrate that the proposed protocol effectively constructs bidirectional channel measurements with high reciprocity, thereby enabling key generation in FDD systems.

References

[1] J. Ding, M. Nemati, C. Ranaweera, and J. Choi, "IoT connectivity technologies and applications: A survey," *IEEE Access*, vol. 8, pp. 67 646–67 673, 2020.

[2] G. Li, A. Hu, C. Sun, and J. Zhang, "Constructing reciprocal channel coefficients for secret key generation in FDD systems," *IEEE Communications Letters*, vol. 22, no. 12, pp. 2487–2490, 2018.

[3] W. Wang, H. Jiang, X. Xia, P. Mu, and Q. Yin, "A wireless secret key generation method based on Chinese remainder theorem in FDD systems," *SCIS.*, vol. 55, pp. 1605–1616, 2012.

[4] B. Liu, A. Hu, and G. Li, "Secret key generation scheme based on the channel covariance matrix eigenvalues in FDD systems," *IEEE Communications Letters*, vol. 23, no. 9, pp. 1493–1496, 2019.

[5] X. Wu, Y. Peng, C. Hu, H. Zhao, and L. Shu, "A secret key generation method based on CSI in OFDM-FDD system," in *2013 IEEE Globecom Workshops (GC Wkshps)*. IEEE, 2013, pp. 1297–1302.

[6] D. Qin and Z. Ding, "Exploiting multi-antenna non-reciprocal channels for shared secret key generation," *IEEE Transactions on Information Forensics and Security*, vol. 11, no. 12, pp. 2693–2705, 2016.

[7] P. Linning, G. Li, J. Zhang, R. Woods, M. Liu, and A. Hu, "An investigation of using loop-back mechanism for channel reciprocity enhancement in secret key generation," *IEEE Transactions on Mobile Computing*, vol. 18, no. 3, pp. 507–519, 2018.

[8] X. Zhang, G. Li, J. Zhang, A. Hu, Z. Hou, and B. Xiao, "Deep-learning-based physical-layer secret key generation for FDD systems," *IEEE Internet of Things Journal*, vol. 9, no. 8, pp. 6081–6094, 2021.

[9] W. Henkel, "Method for physical key generation in frequency division duplexing (FDD)," Aug. 18 2016, DE patent, 102015113730A1.

[10] W. Henkel, O. A. Graur, N. S. Islam, U. Pagel, N. Manak, and O. Can, "Reciprocity for physical layer security with wireless FDD and in wireline communications," in *2018 IEEE Globecom Workshops (GC Wkshps)*. IEEE, 2018, pp. 1–6.

[11] H. L. Van Trees, *Optimum array processing: Part IV of detection, estimation, and modulation theory*. John Wiley & Sons, 2002.

[12] E. O. Torshizi, U. Uprety, and W. Henkel, "Highly efficient fdd secret key generation using esprit and jump removal on phase differences," in *2022 IEEE Conference on Communications and Network Security (CNS)*. IEEE, 2022, pp. 1–6.

[13] A. Rukhin, J. Soto, J. Nechvatal, M. Smid, E. Barker, S. Leigh, M. Levenson, M. Vangel, D. Banks, A. Heckert *et al.*, "A statistical test suite for random and pseudorandom number generators for cryptographic applications-special publication 800-22 rev1a," *Tech. Rep. April*, 2010.